Directional Dependence of the Mean Excitation Energy and Spectral Moments of the Dipole Oscillator Strength Distribution of Glycine and Its Zwitterion

Stephan P. A. Sauer,[†,‡] Jens Oddershede,[§,||] and John R. Sabin*[,§,||]

Department of Chemistry, University of Copenhagen, Universitetsparken 5, DK-2100 Copenhagen, Denmark, Max-Planck-Institute fûr Kohlenforschung, Kaiser-Wilhelm-Platz 1, D-45470 Mûlheim an der Ruhr, Germany, Department of Chemistry, University of Southern Denmark, Campusvej 55, DK-5230 Odense, Denmark, and Department of Physics, University of Florida, Gainesville, P.O. Box 118435, Florida 32611-8435

Received: March 7, 2006; In Final Form: May 25, 2006

In this contribution, we consider the interaction of glycine, a small, model biomolecule, and its zwitterion with fast ion radiation. The object of the study is to determine the differences in properties among various conformers and orientations of the neutral molecule and the zwitterion and to determine if these differences will have implications in terms of radiation protection and radiation therapy. To this end, quantum mechanical calculations were carried out on three conformers of the neutral molecule and two of the zwitterion to determine both the isotropic and directional components of the moments of the dipole oscillator strength distribution in each case. It is these moments that determine the interaction of swift radiation with a molecule.

1. Introduction

The spectral moments of the dipole oscillator strength distribution (DOSD) of a biomolecular system are of considerable interest, as they describe many aspects of the electronic interactions of a biomolecule with its surroundings. The μth moments $S(\mu)$, $L(\mu)$, and I_μ are defined as

$$S(\mu) = \int E^\mu \frac{\mathrm{d}f}{\mathrm{d}E}\,\mathrm{d}E \tag{1}$$

$$L(\mu) = \int E^\mu \ln E \frac{\mathrm{d}f}{\mathrm{d}E}\,\mathrm{d}E \tag{2}$$

and

$$\ln I_\mu = \frac{L(\mu)}{S(\mu)} \tag{3}$$

where E and f label the excitation energies and dipole oscillator strengths of the system, respectively.

The I values are referred to as the mean excitation energies of the system and describe the energy deposition or stopping ($\mu = 0$) and broadening or straggling ($\mu = 1$) in the collision of a swift, massive ion with the target molecule. The mean excitation energies are the target parameters that determine the characteristics of energy deposition, and thus radiation damage, when ionizing radiation interacts with biomolecules.[1] The S moments can be related to other physical properties of a system, such as the Lamb shift ($\mu = 2$), electronic excitations ($\mu = -1$), and the static polarizability ($\mu = -2$).[2]

There has been considerable interest in the spectral moments of smaller molecules over the years,[3] but little attention has been paid to biomolecular systems, with the exception of water. It is the purpose of this contribution to consider the spectral moments of the DOSD of a simple, model, bioorganic molecule and its zwitterions, namely, glycine (NH_2CH_2COOH), and especially the implications for energy deposition and radiation damage to this molecule.

2. Calculations

Structure calculations were first carried out on glycine using density functional theory (DFT),[4] with the B3LYP functional[5] and the 6-31+G(d,p)[6] basis. Geometry optimizations were done starting from several rotamers/conformers, as several local minima are available near to the global minimum, and the starting geometry may determine which of these minima is found by the optimization routine. As the energy minimized geometry depends somewhat on the starting structure, we ran the optimization starting from many different rotamers and report the resulting lowest energy structures. Figure 1 depicts the minimum energy geometry (conformer A), which correlates well with the experimental[7,8] and other theoretical[9] ground-state geometries. We note, however, that we have no guarantee that we have found the true global minimum. The coordinate system is chosen for convenience of comparison among structures. In all cases, the positive x-axis lies along the C−C bond with the C−C−N group in the xy-plane. In conformers A and B, as well as the gas-phase zwitterion conformer, the O−C−O groups are also in the xy-plane, whereas it is slightly twisted out-of-plane in the other conformers.

Conformer A is the most stable neutral structure (theoretically, and experimentally[7] by micro- and millimeter wave rotational spectroscopy). The C−N and O−H bonds are both synperiplanar to the C═O bond. There is, therefore, a bifurcated hydrogen bond from the amino group to the carbonyl oxygen, $NH_2\cdots O{=}C$, as well as a second hydrogen bond (within the carboxyl group) from the hydroxy group to the carbonyl oxygen $OH\cdots O{=}C$.

Conformers B and C in Figure 1 correspond to the two lowest local minimum structures. Conformer B is the least stable of the three neutral structures. The structures have been experi-

* To whom correspondence should be addressed. E-mail: sabin@qtp.ufl.edu.
† University of Copenhagen.
‡ Max-Planck-Institute fûr Kohlenforschung.
§ University of Southern Denmark.
|| University of Florida.

10.1021/jp061412i CCC: $33.50
Published on Web 06/27/2006

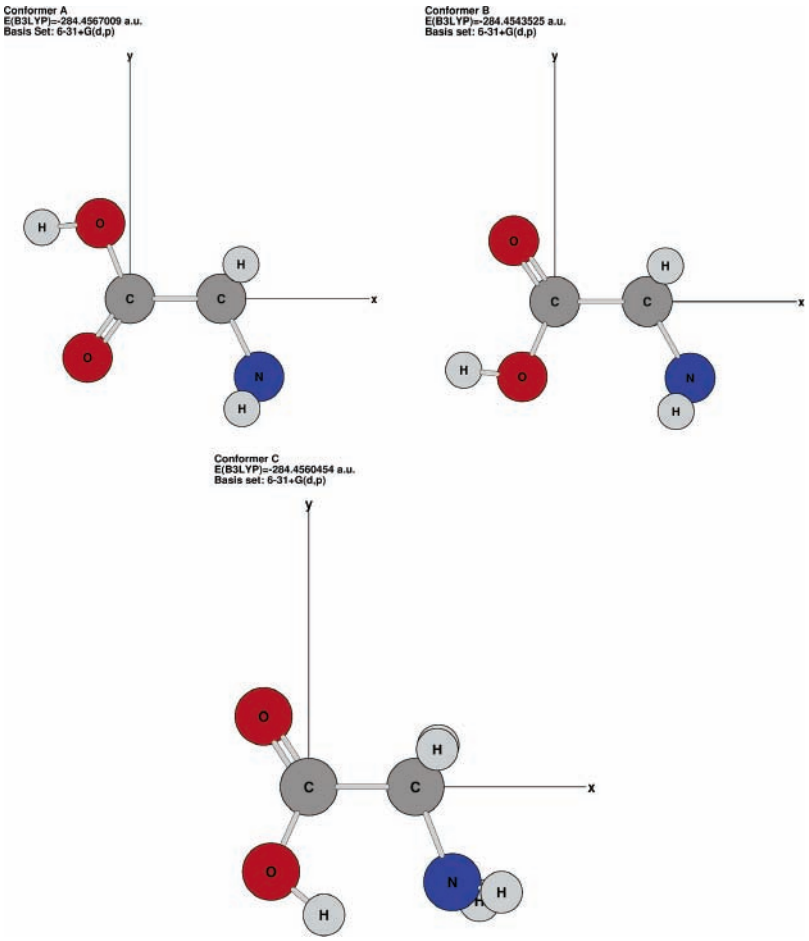

Figure 1. Conformers A, B, and C of glycine. Conformer A is the lowest energy structure.

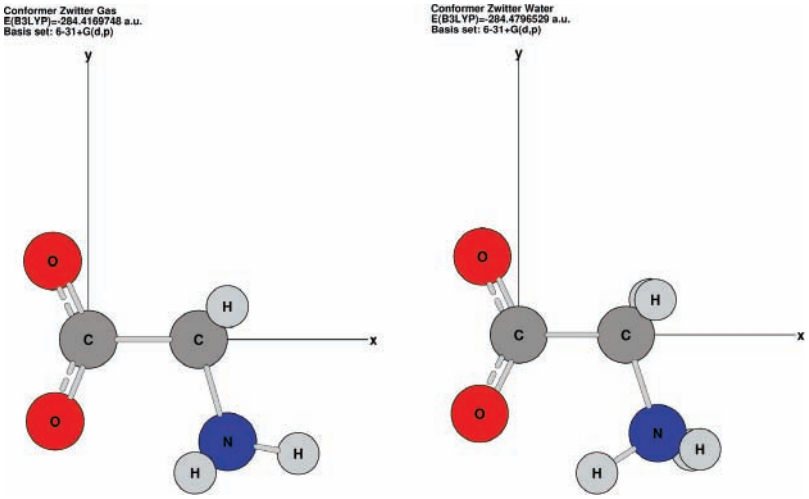

Figure 2. Glycine zwitterions in the configuration determined for the gas state and in water solution.

mentally determined by matrix isolation IR spectroscopy in an Ar matrix below 13 K.[8] The OH and C═O groups are still synperiplanar which implies again a hydrogen bond within the carboxyl group, but the C−N bond is now antiperiplanar to the C═O bond. As a result, there is only a weak bifurcated hydrogen bond between the amino group and the hydroxy group: NH_2··OH.

Conformer C is the second most stable conformation and is also observed in micro- or millimeter wave rotational spectroscopy.[7] Here, the C−N and O−H bonds are antiperiplanar to the C═O bond. Only this structure is converted to the zwitterionic structure: zwitter−water. One notes that the energy difference between the ground state and the lowest local minimum, ΔE_{AC}, is only 0.018 eV or 0.412 kcal/mol.

Similarly, Figure 2 depicts the glycine zwitterion in its gas-phase minimum energy geometry and in the geometry it has when in aqueous solution. The latter was developed from Conformer C using the PCM continuous solvation model[10] as implemented in Gaussian 03.

Once the molecular geometries were established, the electronic structure was calculated,[11] using a method based on the polarization propagator scheme.[12] To evaluate the moments in eqs 1−3, one needs the complete sets of excitation energies $\{E_{0n}\}$ and dipole oscillator strengths $\{f_{0n}\}$ for glycine. These

TABLE 1: Calculation of the Thomas−Reiche−Kuhn Sum for Glycine Using Various Basis Sets[a]

basis	number of functions		$S^L(0)$	$S^V(0)$	I_0 (eV)
6-31G[b]	3s2p/2s	55	21.9	14.7	36.0
6-311G[b]	4s3p/3s	80	26.7	20.4	53.0
6-31+G(d,p)[b]	4s3p1d/2s1p	115	33.9	27.4	43.6
6-311G(2d,2p)[b]	4s3p2d/3s2p	160	36.8	34.9	52.8
6-311++G(2d,2p)	5s4p2d/4s2p	185	36.6	35.3	52.2
Sadlej pVTZ[c]	5sts3p2d/3s2p	165	31.6	31.4	39.1
cc-VTZ[d]	4s3p/3s	80	26.2	19.7	48.9
cc-VQZ[d]	5s4p/4s	105	28.5	23.3	61.1
cc-CVTZ[d]	6s5p/3s	120	31.9	24.4	86.4
cc-CVQZ[d]	8s7p/4s	165	31.4	25.1	83.1
cc-VTZ uncontracted	10s5p/5s	150	31.7	24.6	85.8
cc-VQZ uncontracted	12s6p/6s	180	31.4	25.1	83.8
cc-CVTZ uncontracted	12s7p/5s	190	32.1	24.7	89.7
cc-CVTZ+(3d)[e]	6s5p3d/3s	195	40.0	39.3	72.0
aug-cc-CVTZ+(3d)[f]	7s6p3d/4s	220	40.0	38.8	71.8
cc-CVTZ+(3df) [g]	6s5p3d1f/3s	230	40.1	39.1	71.7
cc-CVTZ+(3d,p)[h]	6s5p3d/3s1p	210	40.1	39.2	71.6
cc-CVTZ+(3d,p)&s+p-recontracted[i]	4s5p3d/3s1p	200	40.0	39.4	70.8
cc-CVTZ+(3d,p)&recontracted[j]	4s5p2d/3s1p	175	39.6	39.2	69.4
cc-CVTZ+(3df,p)&recontracted[k]	4s5p3d1f/3s1p	210	39.6	39.3	69.6

[a] The associated mean excitation energy is also included to illustrate its variation with basis set quality. The *S* moments are pure numbers, and the mean excitation energies are in electronvolts. [b] Reference 6. [c] Reference 15. [d] Correlation-consistent polarized and correlation-consistent polarized core/valence basis sets[16] cc-pVTZ, cc-pVQZ, cc-pCVTZ, and cc-pCVQZ without the polarization functions, that is, without p-, d-, and f-type functions on hydrogen and without the d-, f-, and g-type functions on C, N, and O. [e] Correlation-consistent polarized core/valence triple-ζ basis set cc-pCVTZ[16] without the polarization functions, that is, without p- and d-type functions on hydrogen and without the d- and f-type functions on C, N, and O. Three sets of spherical d-type functions were added to C (with exponents 1.097, 0.318, and 0.1), N (with exponents 1.654, 0.469, and 0.151), and O (with exponents 2.314, 0.645, and 0.214). [f] Augmented correlation-consistent polarized core/valence triple-ζ basis set aug-cc-pCVTZ[16] without the polarization functions, that is, without p- and d-type functions on hydrogen and without the d- and f-type functions on C, N, and O. Three sets of spherical d-type functions were added to C (with exponents 1.097, 0.318, and 0.1), N (with exponents 1.654, 0.469, and 0.151), and O (with exponents 2.314, 0.645, and 0.214). [g] cc-CVTZ+(3d) basis set plus one set of spherical f-type functions added to C (with exponent 0.268), N (with exponent 0.364), and O (with exponent 0.5). [h] cc-CVTZ+(3d) basis set plus one set of p-type functions added to H (with exponent 0.388). [i] cc-CVTZ+(3d,p) basis set with the s- and p-type functions contracted with the contractions coefficients given in Tables 2−5. [j] cc-CVTZ+(3d,p) basis set with the s-, p-, and d-type functions contracted with the contractions coefficients given in Tables 2−5. [k] cc-CVTZ+(3df,p) basis set with the s-, p-, and d-type functions contracted with the contractions coefficients given in Tables 2−5.

are obtained in the dipole length approximation as the residues and poles of the polarization propagator

$$\langle\langle r_a; r_b\rangle\rangle_E = \sum_{n\neq 0}\left[\frac{\langle 0|r_a|n\rangle\langle n|r_b|0\rangle}{E - E_n + E_0} - \frac{\langle 0|r_b|n\rangle\langle n|r_a|0\rangle}{E + E_n - E_0}\right] \quad (4)$$

where r_a is a component of the dipole operator. From the poles ($E_{0n} = E_n - E_0$) and the residues ($\langle 0|\vec{r}|n\rangle$) of the propagator, the oscillator strengths in the dipole length approximation can be calculated

$$f_{0n}{}^{L} = \frac{2}{3}\langle 0|\vec{r}|n\rangle\langle n|\vec{r}|0\rangle (E_n - E_0) \quad (5)$$

Experience has shown that some correlation is necessary to obtain reliable spectral moments of the DOSD, and consequently, we carried out the calculations reported here in the random phase approximation (RPA). (It should be noted that dipole oscillator strengths can be calculated in dipole velocity, dipole length, or mixed representation, depending on which operators are used. In the RPA used here, the result should be identical, if the computational basis were complete.[13,14]) The calculations are carried out using a finite basis set that yields a finite number of excitations equal to the number of particle-hole excitations allowed by the basis. As a result, we approximate the continuum with a finite number of discrete excitations (pseudo-states) placed such that they represent the continuum. We have found that this discretization of the continuum works well when sums over the entire excitation spectrum are taken, but no significance attaches to the individual pseudo-states.

As in RPA, the length [$S^L(0)$] and velocity [$S^V(0)$] forms of the Thomas−Reiche−Kuhn (TRK) sum rule should be identical for a complete basis, the adherence to[13]

$$S^L(0) = S^V(0) = N \quad (6)$$

provides a figure of merit for the basis set used in calculation. For glycine, the total number of electrons is 40, so that the best calculation will be that with the closest agreement of the $S^L(0)$ and $S^V(0)$ moments with that number. We first tried the 6-31+G-(d,p) basis set which was used in the optimization of the structures. But with 33.9 and 27.4 for $S(0)$ in length and velocity representation, respectively, it clearly fails to satisfy the TRK sum rule. We have therefore investigated a large series of standard basis sets (Pople type basis sets,[6] Sadlej's medium size polarized valence triple-ζ basis set,[15] and Dunning's correlation-consistent and correlation-consistent core/valence basis sets[16]) as well our own modifications of them using a preliminary geometry for conformer A. A summary of most of the results is given in Table 1, where we present $S(0)$ and I_0 calculated for conformer A of neutral glycine.

One of the main conclusions of this basis set study is that neither fulfillment of the TRK sum rule nor convergence of the mean excitation energy can be achieved by simply augmenting standard energy optimized valence double and triple-ζ basis sets, 6-31G and 6-311G,[6] with diffuse and polarization functions. Furthermore, Sadlej's medium size polarized basis set,[15] which is optimized for the calculation of dipole polarizabilities, that is, for the $S^L(-2)$ sum rule, gives almost perfect agreement between the $S(0)$ sum rules in length and velocity representation, but the value of the TRK sum rule is not in agreement with the

number of electrons, and the mean excitation energy I_0 is far from converged. This illustrates: (a) that agreement between length and velocity representation is a necessary but by no means a sufficient criterion for the completeness of the basis set and (b) that good reproduction of negative index sum rules such as $S(-2)$ does not guarantee equally good reproduction of $S(0)$. It indicates furthermore that the problem might not be an insufficient number of diffuse or polarization functions but rather the omission of compact core and or valence functions.

Converged results can be obtained within the series of the correlation-consistent or correlation-consistent core/valence basis sets by Dunning and co-workers[16]. However, these basis sets become rather quickly prohibitively large and are furthermore optimized for post-Hartree−Fock methods. Since we have to calculate the whole excitation spectrum and are aiming at larger systems than glycine in the future, we need to use basis sets that are as small as possible. We thus decided to generate a nonstandard basis set optimized for the calculation of $S(0)$ and $L(0)$ based on Dunning's correlation-consistent or correlation-consistent core/valence basis sets guided by our experience obtained in the calculation of mean excitation energies of small molecules.[17,18] First, we have investigated the convergence of the core and valence functions in the basis set. For that purpose, we have removed the polarization functions from Dunning's correlation-consistent polarized valence triple and quadruple-ζ basis sets, cc-pVTZ and cc-pVQZ, as well as their core/valence versions, cc-pCVTZ and cc-pCVQZ. The resulting basis sets are called, cc-VTZ, cc-VQZ, cc-CVTZ, and cc-CVQZ in Table 1. Comparison of the results using these basis sets with those obtained from the totally uncontracted versions shows that the contraction in energy optimized basis sets is not optimal for the calculation of sum rules and in particular mean excitation energies. This is not unexpected because earlier basis set studies for calculations of indirect nuclear spin−spin coupling constants[19] showed also that the contraction scheme in energy optimized basis sets is too restrictive for property calculations. However, adding the core/valence s- and p-type functions to the cc-VTZ or cc-VQZ basis set, that is, the cc-CVTZ or cc-CVQZ basis sets, has almost the same effect as uncontracting the basis set. Further uncontraction of the cc-CVTZ basis set gives only very small additional changes in the TRK sum rules and a small increase in the mean excitation energy. Going to the larger cc-CVQZ basis set, on the other hand, does not significantly change the TRK sum rules and reduces the mean excitation energy by the same amount as uncontracting the cc-CVTZ basis set. We have therefore based our further basis set investigation on the cc-CVTZ basis set.

Adding a set of three polarization functions (d-type functions) to C, N, and O brings the length version of the TRK sum rule in perfect agreement with the number of electrons, whereas adding second polarization functions (f-type functions) on C, N, and O or the addition of extra diffuse s- and p-type functions (in the aug-cc-CVTZ+(3d) basis set) leads to no further changes. The velocity representation of the TRK sum rule, on the other hand, becomes almost fulfilled by adding a set of polarization functions also on hydrogen.

Finally, we have investigated the possibility of reducing the size of the basis set by recontraction with contraction coefficients (see Tables 2−5) optimized for the calculation of TRK sum rules and mean excitation energies. Recontracting the s- and p-type functions has almost no effect on the sum rules and mean excitation energies, whereas contracting also the d-type functions leads to a small change in the length representation of $S(0)$ and in I_0.

TABLE 2: Contraction Scheme for the Hydrogen Basis Set in the cc-CVTZ+(3d,p)&s+p-recontracted, cc-CVTZ+(3d,p)&recontracted, and cc-CVTZ+(3df,p)&s+P+d-recontracted Basis Sets

type	exponents	contraction coefficients		
s	33.87	0.006068		
	5.095	0.045308		
	1.159	0.202822		
	0.3258	0.503903	1.0	
	0.1027	0.383421		1.0
p	0.388	1.0		

TABLE 3: Contraction Scheme for the Carbon Basis Set in the cc-CVTZ+(3d,p)&s+p-recontracted, cc-CVTZ+(3d,p)&recontracted, and cc-CVTZ+(3df,p)&s+p+d-recontracted Basis Sets

type	exponents	contraction coefficients		
s	8236.0000000	0.00053039	−0.00009616	
	1235.0000000	0.00411048	−0.00073384	
	280.8000000	0.02102507	−0.00388514	
	79.2700000	0.08208202	−0.01492588	
	25.5900000	0.23228295	−0.05030603	
	11.8760000	0.02042596	0.03590025	
	8.9970000	0.40422973	−0.16231761	
	4.2920000	0.03866581	0.10233061	
	3.3190000	0.31455823	−0.23112567	
	0.9059000	0.05110149	0.13118148	1.0
	0.3643000	−0.02426862	0.38255332	
	0.1285000	0.00123195	0.09169152	1.0
p	33.1900000	0.00254781		
	18.7100000	0.00388847		
	8.7780000	0.00747443		
	4.1330000	0.05132879	1.0	
	1.2000000	0.19294628		1.0
	0.3827000	0.31564511		1.0
	0.1209000	0.14272280		1.0
d	1.0970000	0.02390918		
	0.3180000	0.03102782		
	0.1000000	0.00727386	1.0	

TABLE 4: Contraction Scheme for the Nitrogen Basis Set in the cc-CVTZ+(3d,p)&s+p-recontracted, cc-CVTZ+(3d,p)&Recontracted, and cc-CVTZ+(3df,p)&s+p+d-recontracted Basis Sets

type	exponents	contraction coefficients		
s	11420.000000	0.00052237	−0.00009931	
	1712.000000	0.00404930	−0.00076776	
	389.300000	0.02072418	−0.00399186	
	110.000000	0.08097449	−0.01583512	
	35.570000	0.23088188	−0.05001146	
	16.201000	0.01947062	0.00818409	
	12.540000	0.40623622	−0.12436409	
	5.952000	0.03217617	0.01407455	
	4.644000	0.32184579	−0.15513058	
	1.293000	0.04795555	0.10615035	1.0
	0.511800	−0.01517467	0.50123660	
	0.178700	−0.00099723	0.18731114	1.0
p	44.849000	0.00245271		
	26.630000	0.00545538		
	11.871000	0.00565961		
	5.948000	0.05952630	1.0	
	1.742000	0.19962019		1.0
	0.555000	0.35241933		1.0
	0.172500	0.18373684		1.0
d	1.654000	0.01221608		
	0.469000	0.02451854		
	0.151000	0.00175787	1.0	

The main conclusion of this basis set study is thus that for a good reproduction of the $S(0)$ and $L(0)$ sum rules one needs both compact core and valence functions in addition to the diffuse and polarization functions necessary for, for example, static polarizabilities $S(-2)$. The optimized basis sets are

TABLE 5: Contraction Scheme for the Oxygen Basis Set in the cc-CVTZ+(3d,p)&s+p-recontracted, cc-CVTZ+(3d,p)&recontracted, and cc-CVTZ+(3df,p)&s+p+d-recontracted Basis Sets

type	exponents	contraction coefficients		
s	15330.000000	0.00050761	−0.00010352	
	2299.000000	0.00393359	−0.00080359	
	522.400000	0.02020158	−0.00416521	
	147.300000	0.07940170	−0.01680503	
	47.550000	0.22886974	−0.05236510	
	21.032000	0.01927424	−0.00355842	
	16.760000	0.40713471	−0.11539093	
	7.845000	0.02874500	−0.02019752	
	6.207000	0.32757525	−0.13431817	
	1.752000	0.04688125	0.11618187	1.0
	0.688200	−0.01128573	0.54849053	
	0.238400	0.00518242	0.27067058	1.0
p	57.437000	0.00273723		
	34.460000	0.00653498		
	15.159000	0.00603795		
	7.749000	0.06890813	1.0	
	2.280000	0.22247282		1.0
	0.715600	0.37580377		1.0
	0.214000	0.16393722		1.0
d	2.314000	0.00516448		
	0.645000	0.02393086		
	0.214000	0.01270063	1.0	

TABLE 6: Directional Components and Total Isotropic *S* Moments of the Dipole Oscillator Strength Distribution for Conformer A of Glycine, in the Dipole Length Formulation and in Hartree Atomic Units

	S_x (m)	S_y (m)	S_z (m)	S (m)
$S(-6)$	569.9	512.3	225.9	436.0
$S(-5)$	254.3	237.6	120.1	204.0
$S(-4)$	124.0	119.7	69.0	104.2
$S(-3)$	67.2	66.7	43.5	59.1
$S(-2)$	41.6	42.1	31.0	38.2
$S(-1)$	31.1	31.6	26.9	29.9
$S(0)$	40.0	39.9	40.1	40.0
$S(1)$	337.2	336.0	343.6	338.9
$S(2)$	12766.4	12774.1	12823.4	12788.0

therefore similar to the basis sets needed for calculation of the diamagnetic contributions to magnetizabilities or nuclear magnetic shieldings in the Geertsen or CTOCD-DZ formulations.[20]

We thus choose the cc-CVTZ+(3d,p)&s+p-recontracted basis as the computational basis, and all further results will be reported using that basis.

3. Results

As molecular orientation has considerable importance in the consideration of the interaction of biological molecules with radiation, it is of interest to determine the anisotropy of a molecule with respect to such an interaction. Such processes as energy deposition by swift ions with the concomitant possibility ionization and fragmentation (I_0) and electronic excitation (I_{-1}) of biomolecules are possibilities.

In Tables 6 and 7, we present the directional components of the *S* and *L* moments of the dipole oscillator strength distribution in the length formulation for conformer A of glycine. It is clear that the in-plane components of the moments are similar (the more so for larger μ), while the out-of-plane component is somewhat different.

A similar observation can be made concerning the mean excitation energies, which are presented in Table 8, again for conformation A and in the length formulation. As expected, the directional mean excitation energies, and especially the I_0 values which govern energy deposition, are nearly identical in the in-plane directions and somewhat different in the perpendicular direction.

TABLE 7: Directional Components and Total Isotropic *L* Moments of the Dipole Oscillator Strength Distribution for Conformer A of Glycine, in the Dipole Length Formulation and in Hartree Atomic Units

	L_x (m)	L_y (m)	L_z (m)	L (m)
$L(-6)$	−482.1	−411.9	−151.0	−348.3
$L(-5)$	−194.6	−173.4	−71.4	−146.5
$L(-4)$	−82.8	−76.4	−35.3	−64.9
$L(-3)$	−37.1	−35.2	−17.7	−30.0
$L(-2)$	−16.7	−16.3	−8.0	−13.7
$L(-1)$	−4.4	−4.7	0.4	−2.9
$L(0)$	37.3	36.4	41.6	38.4
$L(1)$	1069.6	1068.9	1080.7	1073.1
$L(2)$	50302.3	50343.5	50461.3	50369.0

TABLE 8: Directional Components and Total Isotropic Mean Excitation Energies (*I* moment) for Conformer A of Glycine in the Dipole Length Formulation in Electronvolts

	I_m^x	I_m^y	I_m^z	I_m
I_{-6}	11.7	12.2	13.9	12.2
I_{-5}	12.7	13.1	15.0	13.3
I_{-4}	13.9	14.4	16.3	14.6
I_{-3}	15.7	16.1	18.1	16.4
I_{-2}	18.2	18.5	21.0	19.0
I_{-1}	23.6	23.5	27.6	24.7
I_0	69.1	67.7	76.8	71.1
I_1	649.2	655.0	632.2	645.3
I_2	1399.4	1400.6	1392.3	1397.4

5. Discussion and Conclusions

From the foregoing tables, it is clear that the properties of glycine which are derivative of the DOSD have a directional dependence and that, although glycine itself is not symmetric, properties related to the directions defined by the NCC plane are similar, while those related to the direction perpendicular to that plane are somewhat different.

The particular example of interest here is energy deposition. The energy deposition, or stopping power, of a target molecule can be written in the simple Bethe approximation[21] as

$$-\frac{dE}{dx} = n\frac{4\pi e^2 Z_1^{\,2} Z_2}{m\upsilon^2}\ln\frac{2m\upsilon^2}{I_0} \qquad (7)$$

The energy loss per unit path length in a material is related to the velocity, υ, of the projectile and the appropriate mean excitation energy, I_0. Directional stopping is obtained from the proper directional mean excitation energies.[22] Here, Z_1 and Z_2 are projectile charge and target electron number respectively, n is the number density of scattering centers, and the other symbols have their usual meaning. From the differences in the directional mean excitation energies for conformer A, it is clear that the energy deposited in an oriented glycine molecule by a swift ion will depend on the orientational relationship of the ion beam to the molecule. This relation will then determine into which electronic and vibrational states of the molecule energy can be deposited and thus which possible fragmentation channels can be expected.[23,24] Which fragmentation channels are open should be detectable *via* the angular dependence of the fragment distributions and perhaps via IR spectroscopy of the collision fragments. This information, in turn, gives information on possible directions for experimental study for radiation protection and therapy.

We note that electronic excitation of a molecule occurs only for excitations with polarization perpendicular to the direction

TABLE 9: Isotropic Mean Excitation Energies (I_0 in electronvolts) and Their Anisotropies (in units of electrons) for the Various Conformers of Glycine and its Zwitterion, the Dipole Length Formulation, as Well as the Mean Excitation Energy for Straggling, I_1 (in Hartree atomic units), and the First Few Negative, Even, Higher *S* Moments (*vide infra*)

	I_0	A	I_1	$S(-2)$	$S(-4)$	$S(-6)$
conformer A	71.10	3.38	641.18	38.22	104.22	436.03
conformer B	71.08	3.73	641.23	38.23	104.13	437.73
conformer C	71.03	3.35	641.28	38.17	103.65	440.43
zwitterion−gas	70.91	2.65	641.57	39.05	116.31	588.40
zwitterion−water	70.79	2.93	641.83	39.23	118.57	625.27

TABLE 10: Dipole Moments (Debye units) for the Various Conformers of Glycine and its Zwitterions Calculated at the B3LYP/6-31+G(d,p) Level

	μ_x	μ_y	μ_z	μ_{total}
conformer A	−0.51	1.10	0.00	1.21
conformer B	−0.42	−1.91	0.00	1.95
conformer C	5.49	−2.17	0.05	5.90
zwitterion−gas	9.65	−4.62	−0.00	10.70
Zwitterion−water	12.88	−5.39	2.18	14.13

of projectile motion.[25] Thus, we can define[18] a mean excitation energy corresponding to the stopping power orthogonal to the major molecular plane, $I_0^{\text{o}} = (I_0^y I_0^z)^{1/2}$, and one parallel to the plane, $I_0^{\text{p}} = I_0^x$. For conformer A, we find $I_0^{\text{o}} = 72.1$ eV, while $I_0^{\text{p}} = 69.1$ eV. The increasing mean excitation energy corresponds to increasing compactness of the electron density of the target and thus an increased local plasma frequency for the electron density. In this case, the mean excitation energy is largest, and thus the stopping is smallest, orthogonal to the major molecular plane. Thus, one might expect that, for interactions of swift ions with DNA, stopping, and thus damage, would be less for interactions perpendicular to the major base planes, that is, along the axis of the helix, rather than crosswise to it. Another way to look at this is that it is generally observed that the spectrum of pseudo-states polarized perpendicular to the "molecular axis" ($\Pi \leftarrow \Sigma$) has components at higher energies than does the spectrum of pseudo-states polarized along the axis ($\Sigma \leftarrow \Sigma$). This implies that the L sum rule, which is weighted by ln *E*, is larger in the perpendicular direction and thus leads to a larger I_0^{o}. Similar trends are found for several linear molecules and small polyatomics such as CH_2O.[25]

As a biological environment might make a preferred molecular orientation more likely, it becomes of interest to know more about the orientational properties of biomolecules, of which glycine is a prototype.

The isotropic mean excitation energies for the three conformers of glycine and the two conformers of the glycine zwitterions studied here are presented in Table 9. It is clear that, even though there are significant differences in the geometries of the three conformers of glycine, the isotropic mean excitation energies (I_0) are nearly identical. The implication of that is that the DOSD is similar in the three conformers, leading to the conclusion that they will have nearly the same energy deposition properties. Such behavior is not unexpected, as the connectivity of all three conformers is the same. As the stopping for a molecule can be estimated within an accuracy of approximately ±15% using a Bragg-like rule,[26] and all three conformers have the same kind and number of cores and bonds, it would be expected that their energy deposition characteristics would be similar. Similarly, the connectivity in the zwitterions is identical and very close to that of glycine: a single N−H bond in neutral glycine is replaced by an O−H bond in the zwitterion, and these differ by only 10 eV in the bond mean excitation energy.[17] Thus, as expected, it does not appear that there is much difference in the energy deposition properties among all five systems studied. Thus, one would expect only small differences in the energy deposition properties of the glycine conformers and the isolated molecule or solvated forms of the zwitterion. There is no experimental or theoretical value of the mean excitation energy of any of the forms of glycine with which to compare.

Table 9 also presents the anisotropy in the DOSD defined as[18]

$$A = Z_2 \ln \frac{I_0^y I_0^z}{(I_0^x)^2} \tag{8}$$

The anisotropy difference, the difference in the *I* moments of the DOSD between glycine and its zwitterion, is somewhat more pronounced. The largest differences among the different forms of glycine and between glycine and its zwitterion are, however, found in the higher *S* moments of the dipole oscillator strength distributions, some of which are displayed in Table 9. The significant differences in the *S* moments appear for $S(\mu)$, $\mu \leq -3$, of which the even moments can be measured via the frequency-dependent dipole polarizability, $\alpha(\omega)$. The frequency-dependent dipole polarizability may be expanded as: $\alpha(\omega) = \sum_{n=1}^{\infty} \omega^{2n-2} S(-2n)$. The first three terms in the expansion are listed in Table 9. These moments could be measured by making frequency-dependent polarizability measurements and fitting the results to the power series.

Anisotropy is also reflected in the dipole moments of the various conformers under study, calculated at the same level at which the geometries were determined [B3LYP/6-31+G(d,p)]. These are presented in Debye units in Table 10. As is not unexpected, the dipole moments of the conformers indicate that there is little electronic anisotropy in the direction perpendicular to the molecular plane (*z*), and the anisotropy is much greater in the zwitterions than in the neutral molecule. This property should not be difficult to measure.

In Table 9, we also present I_1, the mean excitation energy for straggling,[27,28] which measures the peak width, or statistical fluctuation, of the energy loss of a swift ion passing through matter. As the I_1 values for the various conformers are virtually identical, no differences in the energy deposition profiles are expected among the conformers.

Finally, it should be noted that, although there is considerable difference in the electronic structure of the glycine molecules and their zwitterions parallel to and perpendicular to the main molecular plane, there is considerably less difference in the isotropic properties. In the context of energy deposition and its consequences on radiation protection and therapy, this means that one might use the properties of oriented molecules to their advantage, but there is not enough difference in the properties of the isotropic systems to discriminate among them.

Acknowledgment. This work has been supported in part by an IBM SUR grant to the University of Florida, which support is gratefully acknowledged. S.P.A.S. acknowledges financial support from FNU and the Carlsberg foundation as well as computer time from DCSC. J.R.S. and S.P.A.S. thank Jørgen Schou and Hans Martin Senn for interesting discussions.

References and Notes

(1) Inokuti, M. *Phys. Rev. A* **1975**, *12*, 102.

(2) Hirschfelder, J. O.; Brown, W. B.; Epstein, S. T. *Adv. Quantum Chem.* **1964**, *1*, 255.

(3) Compare, for example, the work of W. J. Meath et al. See also Meath, W. J.; Jahnwar, B. L.; Kumar, A. *Collect. Czech. Chem. Commun.* **2005**, *70*, 1196, and references therein.

(4) Frisch, M. J.; Trucks, G. W.; Schlegel, H. B.; Scuseria, G. E.; Robb, M. A.; Cheeseman, J. R.; Montgomery, J. A., Jr.; Vreven, T.; Kudin, K. N.; Burant, J. C.; Millam, J. M.; Iyengar, S. S.; Tomasi, J.; Barone, V.; Mennucci, B.; Cossi, M.; Scalmani, G.; Rega, N.; Petersson, G. A.; Nakatsuji, H.; Hada, M.; Ehara, M.; Toyota, K.; Fukuda, R.; Hasegawa, J.; Ishida, M.; Nakajima, T.; Honda, Y.; Kitao, O.; Nakai, H.; Klene, M.; Li, X.; Knox, J. E.; Hratchian, H. P.; Cross, J. B.; Adamo, C.; Jaramillo, J.; Gomperts, R.; Stratmann, R. E.; Yazyev, O.; Austin, A. J.; Cammi, R.; Pomelli, C.; Ochterski, J. W.; Ayala, P. Y.; Morokuma, K.; Voth, G. A.; Salvador, P.; Dannenberg, J. J.; Zakrzewski, V. G.; Dapprich, S.; Daniels, A. D.; Strain, M. C.; Farkas, O.; Malick, D. K.; Rabuck, A. D.; Raghavachari, K.; Foresman, J. B.; Ortiz, J. V.; Cui, Q.; Baboul, A. G.; Clifford, S.; Cioslowski, J.; Stefanov, B. B.; Liu, G.; Liashenko, A.; Piskorz, P.; Komaromi, I.; Martin, R. L.; Fox, J. D.; Keith, T.; Al-Laham, M. A.; Peng, C. Y.; Nanayakkara, A.; Challacombe, M.; Gill, P. M. W.; Johnson, B.; Chen, W.; Wong, M. W.; Gonzalez, C.; Pople, J. A. *Gaussian 03*, revision B.05; Gaussian, Inc.: Pittsburgh, PA, 2003.

(5) Lee, C.; Yang, W.; Parr, R. G. *Phys. Rev. B* **1988**, *37*, 785. Becke, A. D. *J. Chem. Phys.* **1993**, *98*, 5648.

(6) Hehre, W. J.; Ditchfield, R.; Pople, J. A. *J. Chem. Phys.* **1972**, *56*, 2257. Clark, T.; Chandrasekhar, J.; Schleyer, P. V. R. *J. Comput. Chem.* **1983**, *4*, 294.

(7) Suenram, R. D.; Lovas, F. J. *J. Am. Chem. Soc.* **1980**, *102*, 7180. Godfrey, P. D.; Brown, R. D. *J. Am. Chem. Soc.* **1995**, *117*, 2019.

(8) Reva, J. D.; Plokhotnichenko, A. M.; Stepanian, S. G.; Ivanov, A. Y.; Radchenko, E. D.; Sheina, G. G.; Blagoi, Y. P. *Chem. Phys. Lett*. **1995**, *232*, 141. Stepanian, S. G.; Reva, J. D.; Radchenko, E. D.; Duarte, M. L. T. S.; Fausto, R.; Adamovicz, L. *J. Phys. Chem A* **1998**, *102*, 1041.

(9) Bludský, O.; Chocholoušová, J.; Vacek, J.; Huisken, F.; Hobza, P. *J. Chem. Phys.* **2000**, *113*, 4629. Senn, H. M.; Margl, P. M.; Schmid, R.; Ziegler, T.; Blöchl, P. E. *J. Chem. Phys.* **2003**, *118*, 1089.

(10) Miertus, S.; Scrocco, E.; Tomasi, J. *Chem. Phys.* **1981**, *55*, 117. Miertus, S.; Tomasi, J. *Chem. Phys.* **1982**, *65*, 239. Cossi, M.; Barone, V.; Cammi, R.; Tomasi, J. *Chem. Phys. Lett*. **1996**, *255*, 327. Cossi, M.; Barone, V.; Robb, M. A. *J. Chem. Phys.* **1999**, *111*, 5295. Cossi, M.; Barone, V. *J. Chem. Phys.* **2000**, *112*, 2427. Cossi, M.; Barone, V. *J. Chem. Phys.* **2001**, *115*, 4708. Cossi, M.; Rega, N.; Scalmani, G.; Barone, V. *J. Chem. Phys*. **2001**, *114*, 5691. Cossi, M.; Scalmani, G.; Rega, N.; Barone, V. *J. Chem. Phys.* **2002**, *117*, 43.

(11) Calculations were carried out using the RPAC program system: Bouman, T. D.; Hansen, Ae. E. *RPAC Molecular Properties Package*, version 9.0; Copenhagen University: Copenhagen, Denmark, 1990.

(12) For a review of the theory and implementation of the polarization propagator method, see Oddershede, J. Jørgensen, P.; Yaeger, D. L. *Comput. Phys. Rep.* **1984**, *2*, 33. Oddershede, J. *Adv. Chem. Phys.* **1987**, *69*, 201.

(13) Harris, R. A. *J. Chem. Phys.* **1969**, *50*, 3947.

(14) Jørgensen, P.; Oddershede, J. *J. Chem Phys*. **1983**, *78*, 1898.

(15) Sadlej, A. J. *Collect. Czech. Chem. Commun.* **1988**, *53*, 1995.

(16) Dunning, T. H., Jr. *J. Chem. Phys.* **1989**, *90*, 1007. Kendall, R. A.; Dunning, T. H.; Harrison, R. J. *J. Chem. Phys.* **1992**, *96*, 6796. Woon, D. E.; Dunning, T. H., Jr. *J. Chem. Phys.* **1994**, *100*, 2975. Woon, D. E.; Dunning, T. H., Jr. *J. Chem. Phys.* **1995**, *103*, 4574.

(17) Sauer, S. P. A.; Sabin, J. R.; Oddershede, J. *Phys. Rev. A* **1993**, *47*, 1123.

(18) Sauer, S. P. A.; Sabin, J. R.; Oddershede, J. *Nucl. Instrum. Methods Phys. Res., Sect. B* **1995**, *100*, 458.

(19) Enevoldsen, T.; Oddershede, J.; Sauer, S. P. A. *Theor. Chem. Acc.* **1998**, *100*, 275. Provasi, P. F.; Aucar, G. A.; Sauer, S. P. A. *J. Chem. Phys.* **2001**, *115*, 1324.

(20) Sauer, S. P. A.; Oddershede, J. In *Nuclear Magnetic Shieldings and Molecular Structure*; Tossel, J. A., Ed.; Kluwer Academic Publisher: Amsterdam, The Netherlands, 1993; pp 351−365. Sauer, S. P. A.; Paidarová, I.; Oddershede, J. *Mol. Phys*. **1994**, *81*, 87. Sauer, S. P. A.; Paidarová, I.; Oddershede, J. *Theor. Chim. Acta* **1994**, *88*, 351. Ligabue, A. Sauer, S. P. A.; Lazzeretti, P. *J. Chem. Phys.* **2003**, *118*, 6830. Ligabue, A.; Sauer, S. P. A.; Lazzeretti, P. *J. Chem. Phys*., submitted for publication.

(21) For a review of energy deposition theory see: Bonderup, E. *Penetration of Charged Particles through Matter*, 2nd ed.; Aarhus University Press: 1981.

(22) See Mikkelsen, H. H.; Oddershede, J.; Sabin, J. R.; Bonderup, E. *Nucl. Instrum. Methods Phys. Res., Sect. B* **1995**, *100*, 451. See also Cabrera-Trujillo, R.; Sabin, J. R.; Deumens, E.; Öhrn, Y. *Adv. Quantum Chem.* **2005**, *48*, 47.

(23) Gutowski, M.; Skurski, P.; Simons, J. *J. Am. Chem. Soc.* **2000**, *122*, 10159. Rak, J.; Skurski, P.; Simons, J.; Gutowski, M. *J. Am. Chem. Soc.* **2001**, *123*, 11695.

(24) Cabrera-Trujillo, R.; Sabin, J. R.; Deumens, E.; Öhrn, Y. In preparation.

(25) Mikkelsen, H. H.; Oddershede, J.; Sabin, J. R.; Bonderup, E. *Nucl. Instrum. Methods* **1995**, *100*, 458.

(26) Oddershede, J.; Sabin, J. R. *Nucl. Instrum. Methods Phys. Res., Sect. B* **1989**, *42*, 7.

(27) Fano, U. *Annu. Rev. Nucl. Sci.* **1963**, *13*, 1.

(28) Inokuti, M.; Dehmer, J. L.; Baer, T.; Hanson, J. D. *Phys. Rev. A* **1981**, *23*, 95.